

Magnetic properties of self-assembled interacting nanoparticles

D. Kechrakos^{a)} and K. N. Trohidou

Institute of Materials Science, NCSR "Demokritos," 15310 Athens, Greece

(Received 17 July 2002; accepted 21 October 2002)

The temperature-dependent magnetization and the hysteresis properties (remanence and coercivity) of magnetic nanoparticle arrays are studied by Monte Carlo simulations. An oscillatory variation of the remanence with layer coverage and accompanying peaks in the coercive field are predicted at low temperatures, due to dipolar interparticle interactions. The blocking temperature of the arrays decreases with the inverse cube of the interparticle spacing ($T_b \sim d^{-3}$) and it remains almost unchanged with film thickness above one monolayer. Our results are compared with recent experiments on self-assembled Co nanoparticle arrays. © 2002 American Institute of Physics.

[DOI: 10.1063/1.1528290]

Ordered arrays of magnetic nanoparticles¹⁻⁴ and patterned magnetic media⁵ are currently the most promising materials for exploitation in high-density (~ 1 Tb/in²) magnetic storage media, due to the sharp distribution of their magnetic properties and their high reproducibility. Nanoparticle arrays (or superlattices) are prepared by colloidal synthesis followed by size-selective precipitation that produces a very narrow particle size distribution ($\sigma < 5\%$). The latter is a prerequisite for self-assembling of the nanoparticles dispersions on a substrate and ultimate formation of the superlattice. In addition to their technological applications, nanoparticles superlattices are the ideal system for studying the magnetization reversal mechanism in the presence of interparticle interactions, due to the precise knowledge and control of the particle size and interparticle distances. Recent studies of self-assembled arrays of magnetic nanoparticles have provided clear evidence that interactions between the nanoparticles are present and manifest themselves in various aspects of their magnetic behavior. In particular, anisotropy between the in-plane and normal-to-plane remanence magnetization,⁶ distribution of energy barriers with a larger width than the corresponding particle volume distribution,⁷ and flat field-cooled magnetization curves⁴ have been observed and attributed to interparticle dipolar interactions.

The preparation of self-assembled nanoparticles films from colloidal dispersions introduces uncontrollable structural defects at the mesoscopic scale (superlattice geometry). Electron microscopy has provided clear evidence for incomplete monolayer (ML) coverage (voids)^{6,8} and the presence of an unfinished uppermost ML.^{3,4,9} The morphology of the uppermost ML is characterized by random occupation of the underlying hexagonal lattice sites and, under certain circumstances, by formation of terraces along a symmetry axis of the superlattice.³ Provided that the highly reproducible behavior of self-assembled systems is the cornerstone for their potential applications, it is of crucial importance to understand the modifications of their magnetic behavior due to the presence of uncontrollably generated structural defects. Here we present a computer simulation study of the hysteresis characteristics and the temperature-dependent magnetization

of interacting nanoparticle arrays with structural defects at the mesoscopic scale.

We consider identical spherical particles with diameter D forming a two-dimensional triangular lattice in the xy -plane, and lattice constant $d \geq D$. We construct a nanoparticle-assembled film with finite thickness (1–4 ML) by placing particles in the upper layer above alternate interstices in the lower one.^{3,4} Structural defects are considered only in the uppermost ML, and they arise in one of two ways: (i) random occupation of the uppermost layer sites, or (ii) formation of terraces with finite width (w) and orientation along a symmetry axis of the triangular lattice. The particles are single-domain, they possess uniaxial anisotropy in a random direction, and they interact via dipolar forces. The total energy of the system reads:

$$E = g \sum_{i,j} \frac{(\hat{S}_i \cdot \hat{S}_j) - 3(\hat{S}_i \cdot \hat{R}_{ij})(\hat{S}_j \cdot \hat{R}_{ij})}{R_{ij}^3} - k \sum_i (\hat{S}_i \cdot \hat{e}_i)^2 - h \sum_i (\hat{S}_i \cdot \hat{H}), \quad (1)$$

where \hat{S}_i is the magnetic moment direction (spin) of particle i , \hat{e}_i is the easy axis direction, R_{ij} is the center-to-center distance between particles i and j , measured in units of the lattice constant d , and hats indicate unit vectors. The energy parameters entering Eq. (1) are the dipolar energy, $g = \mu^2/d^3$, where $\mu = M_s V$ is the particle moment, $k = K_1 V$ is the anisotropy energy, and $h = \mu H$ is the Zeeman energy due to the applied field H . For Co nanoparticles with hcp or fcc atomic lattice structure, typical values⁶ are $K_1 \sim 10^6$ erg/cc and $M_s \sim 10^3$ emu/cc that give $g/k \sim 0.52(D/d)^3$, while ϵ -Co nanoparticles are soft,⁸ and a ratio $g/k > (D/d)^3$ is considered. The magnetic configuration under an applied field H and finite temperature T was obtained by a Monte Carlo simulation, using the standard Metropolis algorithm.¹⁰ At a given temperature and applied field, the system was allowed to relax towards equilibrium for the first 10^4 Monte Carlo steps per spin, and thermal averages were calculated over the subsequent 10^3 steps. Simulations were performed on a $L \times L \times L_z$ cell with $L = 15d$ and $d_z \leq L_z \leq 4d_z$, where $d_z = d\sqrt{2/3}$ is the interlayer distance. We used periodic boundaries in the xy -plane and free boundaries in the z -axis. The

^{a)}Electronic mail: dkehrakos@ims.demokritos.gr

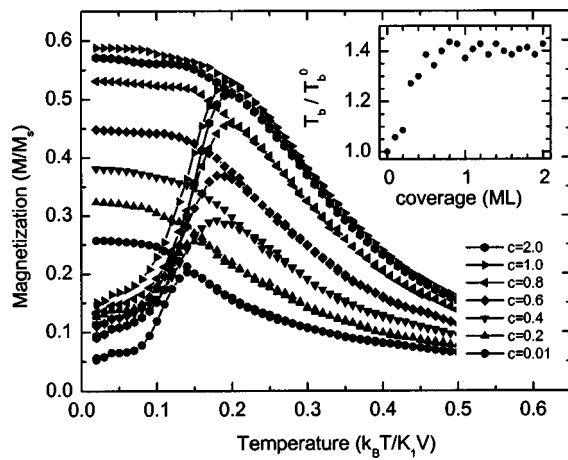


FIG. 1. Dependence of ZFC/FC magnetization on layer coverage for hard Co nanoparticles ($g/k=0.25$). Top layer is randomly occupied. In-plane applied field $h/k=0.1$. Inset shows the dependence of blocking temperature on monolayer coverage.

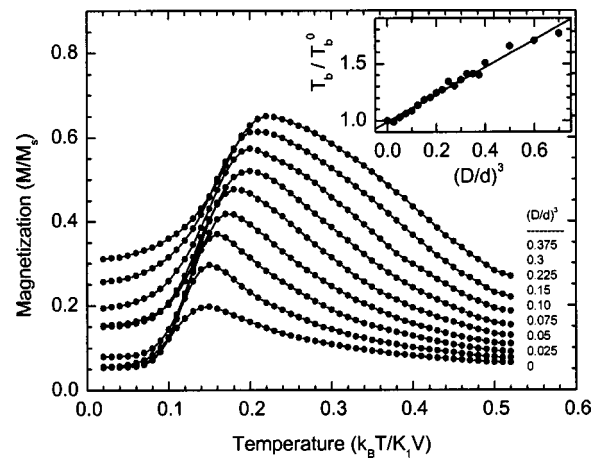


FIG. 2. Dependence of ZFC magnetization on interparticle distance for hard Co nanoparticles ($g/k=0.25$). Uppermost layer is randomly occupied. In-plane applied field $h/k=0.1$. Inset shows the scaling behavior of blocking temperature with interparticle distance.

dipolar interactions were treated without truncation using the Ewald summation method for a quasi-two-dimensional system.¹¹

In Fig. 1 we show the zero-field-cooled (ZFC) magnetization curves for various coverage (c) values and parameters corresponding to hard Co nanoparticles. The maximum of the ZFC curve appears at the blocking temperature (T_b) of the system.¹² An obvious increase of the blocking temperature with layer coverage is seen, that almost reaches saturation as soon as the first complete ML is formed ($c=1$). The increase of T_b with coverage, below 1 ML, is due to the anisotropic and ferromagnetic character of dipolar interactions that introduce an additional barrier to the magnetization reversal of the particles. The increase of T_b with particle concentration has also been observed in granular films.¹²⁻¹⁴ Increased T_b values relative to the dilute limit have been recently measured in self-assembled Co nanoparticle arrays prepared from colloidal dispersions³ and in self-organized lattices of Co clusters in Al_2O_3 matrix.¹⁵ However, in the latter experiments the saturation of T_b values was found after 5-7 layers, while in close-packed hexagonal arrays we demonstrate that saturation occurs already after two layers. Thus, we conclude that in hexagonal closepacked spherical Co particles, the collective behavior is predominantly determined by the intralayer dipolar interactions, while interlayer interactions play only a secondary role.

A strong dependence of the T_b on the interparticle distance (d) is shown in Fig. 2. Our data indicate that for hard magnetic nanoparticles ($g/k < 1$) the blocking temperature scales with the inverse cube of the interparticle distance, $T_b \sim (D/d)^3$. Bearing in mind that the dipolar strength is $g \sim (D/d)^3$, we obtain $T_b \sim g$, which means that in hexagonal arrays of magnetically hard nanoparticles, the dipolar interactions provide an additional energy barrier for magnetization reversal that is proportional to the dipolar coupling strength. To investigate further, the effects of dipolar interactions on the saturation remanence (M_r) and the coercive field (H_c) for strongly dipolar nanoparticle arrays at very low temperature are shown in Fig. 3. The most pronounced feature in these data is the oscillatory dependence of M_r and H_c on the layer coverage. In an ideal hexagonal monolayer,

dipolar interactions produce a ferromagnetic ground state with the magnetization lying along one of the three symmetry axes of the triangular lattice.¹⁶ Successive monolayers are coupled ferromagnetically, and therefore the remanence is always close to unity when the system consists of an integer number of monolayers [Figs. 3(a), 3(b)]. The remanence reaches a minimum every time the uppermost layer is approximately half covered. Upon examination of the layer-resolved magnetization (not shown here) as successive layers are covered, the following picture arises: at low coverage of the top layer ($c_{top} \sim 0-0.2$), small clusters of neighboring nanoparticles exist for which the intralayer coupling dominates over the coupling to the monolayers below. This 2D random dipolar system is frustrated, thus reducing the overall magnetization. At $\sim 50\%$ coverage, the percolation limit for the triangular lattice is reached, and above this coverage the ferromagnetic ground state of the triangular lattice develops. This procedure is repeated for every new monolayer added to the stacking sequence. The amplitude of the magnetization oscillations decays with film thickness because the uppermost layer, which is responsible for the oscillations, consti-

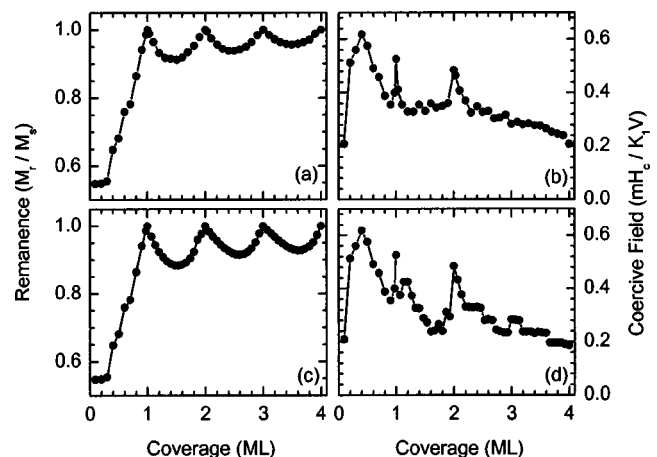


FIG. 3. Dependence of saturation remanence and coercive field on monolayer coverage for soft Co nanoparticles ($g/k=10$) at very low temperature. The in-plane applied field lies along a symmetry axis of the lattice. (a) and (b) Hexagonal close-packed nanoparticles with a random top layer. (c) and (d) Hexagonal close-packed nanoparticles with a terrace on the top layer.

tutes a decreasing fraction of the total volume. Peaks in the coercive field accompany the maximum values of the remanence. In other words, the nanoparticle array is magnetically harder when it consists of ideal monolayers, and a substantial softening is observed even with a few ($\sim 10\%$) voids in the top monolayer. The maximum of the coercive field for $c = 0.5$ ML is attributed to the maximum anisotropy that the system develops around the percolation threshold.¹³ Notice, finally, that the coercive field decreases continuously with film thickness and the peaks are suppressed after a few monolayers thickness, indicating a transition from a 2D to a 3D magnetization reversal mode.

The growth mode of the uppermost monolayer modifies only quantitatively the oscillatory behavior. Thus, if the growth proceeds with formation of terraces,³ similar oscillations are observed in the remanence and corresponding peaks in the coercive field [Figs. 3(c), 3(d)]. In this case, we model the monolayer growth by considering a stripe of nanoparticles on the uppermost layer. The width (w) of the stripe grows by addition of extra rows of nanoparticles, one at a time, until the surface of the film is covered. As in the case of randomly dispersed nanoparticles, minima in the remanence occur when nearly half of the layer is covered by the stripe. However, it is the magnetic domain formation within the stripe that reduces the total magnetization, as opposed to frustrating interactions in the case of a random surface. Examination of the magnetic configuration at remanence shows that the step configuration evolves from a single domain along the stripe axis when the terrace is very narrow ($w \sim 1d - 2d$), to an S-state configuration¹⁷ at intermediate widths ($w \sim 0.5L_x d$), and finally, for wider stripes ($w \sim L_x d$), to a single domain along the magnetization direction of the layers underneath. This evolution of the magnetic configuration of the terrace arises from the competition between the demagnetizing field due to the free edges of the terrace, which tends to align the moments along the edges, and the dipolar coupling to the underlying ferromagnetic monolayer.

In summary, we have investigated the impact of layer coverage and interparticle distance on the magnetic properties of hexagonal arrays of Co nanoparticles due to dipolar interparticle interactions. We demonstrated via Monte Carlo simulations that the blocking temperature: (i) increases with the coverage of the first monolayer and is rather insensitive to additional monolayers and (ii) decreases proportionally to the cube of the interparticle distance ($T_b \sim 1/d^3$). At low temperatures and strongly dipolar samples, as for example, the soft ϵ -phase of Co,⁸ the remanence and the coercive field exhibit an oscillatory dependence on layer coverage with

maximum values at full monolayer coverage, indicating a collective behavior. Our results are in qualitative agreement with recent measurements of ZFC/FC curves,^{3,15} indicating an increase of T_b relative to the dilute limit. More measurements in samples with different surfactants, which allow the interparticle distance to be adjusted,¹⁸ would help to verify the scaling behavior of T_b . Control of the layer coverage could presently be accomplished by variation of the colloidal dispersion concentration.⁴ Our results could motivate more measurements in samples with controlled layer coverage, which will further elucidate the role of dipolar interparticle interactions in nanoparticles assemblies. Finally, the oscillatory behavior demonstrated here for the remanence and coercive field at low temperature is the combined outcome of dipolar interactions and the morphology of the samples at a mesoscopic scale. It is therefore anticipated that similar oscillations could occur in superlattices of magnetic anti-dots, where magnetostatic interactions exist between the magnetic dipoles formed by the free poles formed at each anti-dot.

This work has been supported by the GROWTH project No. G5RD-CT-2001-00478.

- ¹C. Petit, A. Taleb, and M. P. Pileni, *Adv. Mater.* **10**, 259 (1998).
- ²J. M. Harrell, S. Wang, D. E. Nikles, and M. Chen, *Appl. Phys. Lett.* **79**, 4393 (2001).
- ³C. B. Murray, S. Sun, H. Duyle, and T. Betley, *MRS Bull.* **26**, 985 (2001).
- ⁴V. F. Puentes, K. M. Krishnam, and A. P. Alivisatos, *Appl. Phys. Lett.* **78**, 2187 (2001); *Science* **291**, 2115 (2001).
- ⁵R. L. White, *J. Magn. Magn. Mater.* **242–245**, 21 (2002).
- ⁶V. Russier, C. Petit, J. Legrand, and M. P. Pileni, *Phys. Rev. B* **62**, 3910 (2000).
- ⁷S. I. Woods, J. R. Kirtley, S. Sun, and R. H. Koch, *Phys. Rev. Lett.* **87**, 137205 (2001).
- ⁸S. Sun and C. B. Murray, *J. Appl. Phys.* **85**, 4325 (1999).
- ⁹C. T. Black, C. B. Murray, R. L. Sandstrom, and S. Sun, *Science* **290**, 1131 (2000).
- ¹⁰K. Binder and D. W. Heermann, *Monte Carlo Simulation in Statistical Physics*, Springer Series in Solid-State Sciences Vol. 80 (Springer, Berlin, 1988).
- ¹¹A. Grzybowski, E. Gwóźdź, and A. Bródka, *Phys. Rev. B* **61**, 6706 (2000); E. Lomba, F. Lado, and J. J. Weiss, *Phys. Rev. E* **61**, 3838 (2000); G. T. Gao, X. C. Zeng, and W. Wang, *J. Chem. Phys.* **106**, 3331 (1997).
- ¹²J. L. Dormann, D. Fiorani, and E. Tronc, *Adv. Chem. Phys.* **98**, 283 (1997).
- ¹³D. Kechrakos and K. N. Trohidou, *Phys. Rev. B* **58**, 12169 (1998).
- ¹⁴R. W. Chantrell, N. Walmsey, J. Gore, and M. Maylin, *Phys. Rev. B* **63**, 024410 (2000).
- ¹⁵F. Luis, F. Petroff, J. M. Torres, L. M. García, J. Bartholomé, J. Carrey, and A. Vaurès, *Phys. Rev. Lett.* **88**, 217205 (2002).
- ¹⁶V. Russier, *J. Appl. Phys.* **89**, 1287 (2001).
- ¹⁷Y. Zheng and J.-G. Zhu, *J. Appl. Phys.* **81**, 5471 (1997).
- ¹⁸S. Sun, C. B. Murray, D. Weller, L. Folks, and A. Moser, *Science* **287**, 1989 (2000).